Collapse/subsidence : role and influence of overburden in Lorraine iron mines case

Jérôme Fougeron, Mountaka Souley, Françoise Homand

COLLAPSE/SUBSIDENCE: ROLE AND INFLUENCE OF OVERBURDEN IN LORRAINE IRON MINES CASE

FOUGERON Jérôme[1], SOULEY Mountaka[2], HOMAND Françoise[1]

[1] LAEGO, Rue du Doyen Marcel Roubault – BP 40 – 54501 Vandoeuvre-lès-Nancy Cedex - France; jerome.fougeron@ensg.inpl-nancy.fr; francoise.homand@ensg.inpl-nancy.fr

[2] INERIS, Ecole des Mines - 54042 Nancy Cedex - France.; mountaka.souley@ineris.fr

ABSTRACT: This paper presents several large-scale numerical modellings of valley and tray situations with the presence or not of vertical fractures. Through these modellings, we firstly attempt to evaluate an influence zone, in terms of stress variations induced by the creation of the valley. Next we study more particularly the behaviour of a stiff overburden, according to situations, with the aim to estimate if a valley and/or the presence of subvertical fractures influence the overburden massivity.

KEYWORDS: Overburden, stiffness, stress, displacement, energy

RESUME: Ce papier présente plusieurs modélisations à grande échelle d'une situation de vallée et de plateau en présence ou non d'une fracturation verticale. A travers ces modélisations, nous tentons d'évaluer une zone d'influence, en termes de variations de contraintes induites par la création de la vallée. Puis nous étudions plus particulièrement le comportement d'une couverture raide, en fonction des situations, dans l'objectif d'estimer si une vallée et/ou une fracturation subverticale influencent la massivité du recouvrement.

MOTS-CLEFS: Couverture, raideur, contrainte, déplacement, énergie

1. Introduction

In the past, Lorraine was an important mining region leaving many empty spaces in the underground, responsible for many accidental movements. Currently 16 historical cases were recorded in the Lorraine iron ore basin, in particular 8 violent collapses and 8 progressive subsidences. It is important to distinguish violent collapses of progressive subsidences, implications in terms of person security being very different. Consequently, it is necessary to unequivocally define the meaning of these qualifiers as presented to the experts:

A collapse is qualified as violent when the four following criteria below are filled:

1. The collapse follows a seismic event of sufficient magnitude to be recorded at the Institut de Physique de Globe de Strasbourg or, for older collapses, to be felt by the population on the surface ;
2. The event results in an air blast within the mine workings ;
3. After the collapse, the surface profile is very steep and stepwise at the collapse edge ;
4. The collapse is complete in a very short amount of time (less than an hour).

A subsidence is qualified progressive if:

1. The surface profile is gradual at the subsidence edge ;
2. No seismic event precedes the subsidence ;
3. The subsidence occurs over the course of several hours instead of several minutes.

For many years, we attach an importance to the knowledge of these events and mechanisms, which are the cause of instabilities, in order to be able to prioritize them in terms of risk and in this particular case to try preventing them.

Tincelin and Sinou (1962) have proposed like collapse mechanisms:

1. A violent failure of overburden by splitting of a monolithic slab solicited in flexion
2. An overburden failure by shear of bedrock (presence of a thick and competent layer). They suppose that it is the failure of this bedrock, with a high stiffness and a high mechanical strength, which would immediately cause the failure of block rocks.

These explanations are probably too idealized and require to be re-examined on the basis of new geomechanical data and appropriate numerical modellings. Thus, in the iron ore basin, a methodological study of mining risk was led.

2. Discrimination methodology

The sixteen historical subsidence and collapse cases have ended in a methodology allowing to discriminate the both events through different criteria. There are two criteria, the one called *geometrical criterion* ant the other named *geological criterion*.

2.1. Geometrical criterion

The geometrical criterion is expressed by a discriminating function which takes into account the exploitation geometry. Ten quantitative variables were used in both PCA (Principal Component Analysis) and DFA (Discriminating Factorial Analysis) analyses.. These analyses have allowed to put in evidence a certain number of variables (extraction ratio, vertical stress in pillar, overburden thickness, mining height, pillar dimension, room dimension, surface area pillar, hydraulic radius, height-to-width ratio, abutment effect) defining the discriminating function showed on figure 1 (Thoraval, 2000).

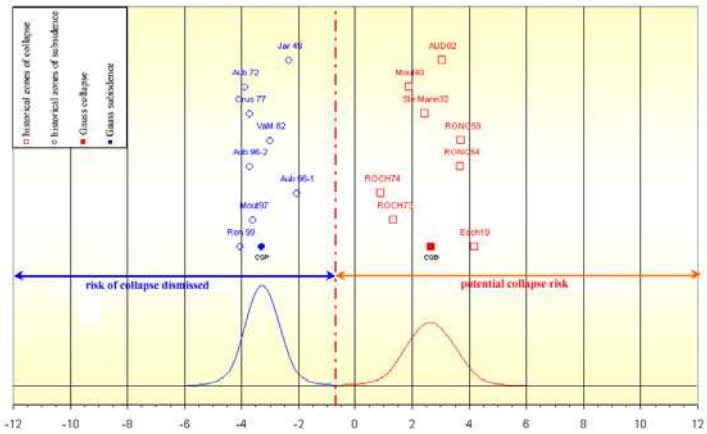

Figure 1: Discriminating function based on geometric criterion

At this stage, it was decided that for a violent collapse alea is retained, it is necessary that the discriminating function value is higher than -0.7 and it has to have the presence of stiff bedrock in the overburden. It allows the affectation of new zones to the one or the other groups without ambiguity when the projection is close to the two gravity centres.
On the other hand, this affectation becomes more delicate when the zone is projected very far from the two centres, indeed impossible when it is near to the centre. This type of analyse shows its insufficiency when we are near the critical discriminating value.

2.2. Geological criterion

For zones, where the doubt can persist, analysis based on a geological criterion is essential. A methodological study was undertaken by an expert group, based on a large geomechanical characterisation of overburden formations in the vicinity of already collapsed zones and/or zones associated a progressive subsidence (Homand, 2004). This consists of four parts:

1. to define facies-types and to emphasize the presence of a homogeneous bedrock « *in the sense of the predominant lithological facies* » with the help of geotechnical core drillings analysis ;
2. to identify the mechanical parameters from laboratory tests (average compressive strength, average Young's modulus,) for each facies-type in order to lead to an overburden characterization in the vicinity of core drillings on the base of the maximum ID value, average RQD and joint type;
3. to calculate the RMR and GSI index, for each unity, in order to evaluate of the deformability modulus at the site scale based on the well known methodologies (Barton 1980, Hoek & Brown 1982, Bieniawski 1989 and Hoek & Brown 1997) ;
4. to propose a stiff index IM.

From this large geomechanical characterisation, the total index expressing the stiffness overburden is defined by Bennani et al. 2004:

$$IM = (2A + B + \frac{C}{2}) \times \frac{f_{disc} + 5}{10} \quad (1)$$

where index A represents the total overburden behaviour by considering only stiff formations, index B is the maximal stiffness bedrock. The geometrical criterion (f_{disc}) is taken into account by the discriminating function.
Formation massivity can be defined like its total stiffness. It bases on the stiffness bedrock concept, which is not an intrinsic characteristic, but which must be evaluated in both morphological (slope, tray, etc.) and geological (fracturing, fault) contexts. The index C takes into account these criteria at a large scale. This corresponds to a morphological index describing four distinct situations encountered in the Lorraine iron basin: promontory, valley, tray and postponed valley.
Initially and hypothetically, it was decided that a tray situation would have a tendency to increase the overburden massivity by the fact that the fracture would be badly expressed imposing limited displacements (index C is equal to 1). On the contrary, it was assumed that the empty space, created by the valley, would reduce the overburden stiffness (index C is equal to 0). These basic premises must be confirmed through a large-scale numerical modelling.

3. Geomorphological large-scale numerical modelling

The tray and valley situation with the presence or not of vertical fracture will be more particularly examined. We will examine at until which distance the valley excavation involves a disturbance of the stress field in the rock mass, the consequences on the stresses and displacements in the overburden and along the horizontal discontinuities (with or not exploitation in depth) and which role play the vertical fracture in the overburden. Finally, displacements and stresses examined in the overburden and in different configurations will be expressed into terms of massivity.
To answer of these questions, numerical modelling simulations are undertaken, which are based on the distinct element code (UDEC) within each discontinuity (interbed and vertical joints) is explicitly taken into account. The influence of numerous parameters (such as stiffness of overburden beds, mechanical properties of discontinuities, presence of vertical fractures etc.) is examined on the basis of a typical geological cross section representing both tray and valley configurations (mean dip at regional scale is 10°).

3.1. Geometrical model and loading sequences

With the aim of to more realistically represent the overburden with a stiff character (typically as certain zones in the basin), the model is basically consisted of stiff facies-types (Figure 2) : Jaumont limestone (stiff), Polypiers 1 limestone (stiff), Polypiers 2 limestone (soft), Polypiers 3 limestone (stiff), Haut-Pont limestone (stiff), Ottange limestone (soft) and Charennes marl (soft). Below marls, there is the iron layer made up of immediate roof (10 m), three iron layers (3.5 m) separated from internal waste (6.5 m) composed of limestone-marl alternation. Geologically, below the iron formation, there is the presence of marls known inferior. Between the last ore exploited layer and

the inferior marls, it has been introduced an additional layer with a power of 10 m which expresses the alternation of marls (very bad quality) and different layers of ore.

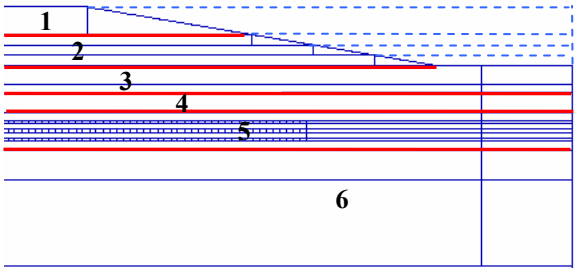

1 : Jaumont limestone 32 m (JCB)
2 : Polypiers limestone 12 m x 3 (PCGC+PCEAM+PCB)
3 : Haut-Pont (HPC) 22 m and Ottange (OTC) limestone 10 m
4 : Charennes marl 22 m (MC)
5 : iron formation
6 : inferior marl

Figure 2: Geological model

The valley formation causes the excavation of large blocks (23270 m^3 corresponding to 1100 m large and 70 m high. Few precautions about the model geometry choice must be taken into consideration. Based on several works reported in the literature, focussed on the model dimensioning in large scale slope modellings (Merrien-Soukatchoff et al. 2001) and in order to have coherent results in terms of stresses and displacements (without boundary effects), the model is 5650 m large on 2750 m high.
The vertical stress is given by the weight of overburden: $\sigma_v = \gamma\ h$. The modelling sequences are performed as follows: firstly, the model without excavation is consolidated under in situ stresses. Secondly, no horizontal displacements on the left side limit are imposed (expressing the no influence of the valley and future works to this limit) and the valley is excavated. Thirdly no displacements on the left side limit are conserved and rooms are excavated.

3.2. Mechanical properties

All materials have an average density, ρ, of 2500 $kg.m^{-3}$. For Poisson's ratio, we consider 0.3 for marls and 0.25 for limestone formations. For overburden limestone, the determination of various characteristics is based on laboratory tests. Modulus (E_m) and strength properties (C_m, ϕ_m) correspond to the rock mass scale and then fractures are already integrated. We use E_m calculated according to Hoek & Brown 97 formulation because it gives highest values, in accordance with our purpose to highlight the "stiff bedrock" role. For Charennes marls properties, it is impossible to apply Hoek & Brown 97 methodology, the spacing between each fracture not having significance. Therefore, the calculation of RMR index is impossible. We agreed to take, on the whole of geomechanical tests, the lowest measured values from laboratory tests.
Upper wall characteristics (ore layers) are equal to 75% of the formation representing the marls and not exploited ore alternation. Mechanical properties of marls at the immediate floor have weak characteristics representing the ore succession and marl internal waste of very poor qualities. They have the third of Charennes marls properties.
Inferior marls have the same characteristics of the iron formation. Finally the inferior part (or model base) is defined as being a resistant unity with mechanical characteristics four times stronger than the iron formation. Table 1 summarizes the input mechanical properties used.

Table 1: Mechanical properties

	E_m (MPa)	K (MPa)	G (MPa)	C_m (MPa)	Φ_m (°)	R_t (MPa)
JCB	21938	14625	8775	1.3	60	0.5
PCGC+PCB	26073	17382	10429	1.7	55	0.5
PCEAM	3897	2598	1559	0.5	33	0.1
HPC	25155	16770	10062	2.3	54	0.5
OTC	4690	3127	1876	0.8	29	0.2
MC	6000	5000	2308	1.0	30	0.5
Roof (immediate)	5860	3905	2343	0.9	26	0.06
Ore	7811	5207	3124	1.2	35	0.08
Marl at immediate floor	4000	3330	1538	0.7	20	0.4
Inferior marls	7811	5207	3124	-	-	-
Base	31244	20828	12496	-	-	-

3.3. Joint characteristics

Unlike the rock mass properties, it was not possible to deduct in advance the mechanical properties of joints. Therefore, the choice of these parameters presented here is based on some approaches encountered in the literature. The normal and shear stiffness K_n and K_s during the consolidation were calculated based on study reported by Kulatilake et al. (1992). In this approach, K_n and K_s depend essentially on the elastic properties of rock materials. Concerning K_n and K_s needed during excavation, it is clearly established that the mechanical behaviour of joints is generally non-linear and depend on large parameters such as: stress level, dilatancy, strength and deformability of asperities. Based on the relationships suggested by Bandis et al. (1983) and assuming that all joints have no dilatancy and their compressive strength (JCS) is equal to the uniaxial compressive strength of rock materials, the initial normal stiffness, the maximum normal closure and the shear stiffness for each discontinuity were calculated. Therefore it is possible to derive the normal stiffness (K_n) according to the normal stress level and the hyperbolic model of Bandis et al.(1983). As a first approach, we assumed that normal and shear behaviours of joints are linear and the shear stress is limited by Mohr-Coulomb criterion.

4. Influence of joint stiffness during the valley formation

Geologically, various joints, which separate formations in the overburden, can be filled with more or less clayey or marly materials. According to this filling, joints will have a more or less stiff behaviour, and both in the normal and tangential direction. For expressing this lithology in discontinuities, several sets of stiffnesses were assigned to joints: « $K_{ns\ ++}$» (« $K_{ns\ base}$ » x 100), « $K_{ns\ +}$» (« $K_{ns\ base}$ » x 10), « K_{ns} » (« $K_{ns\ base}$ »), « $K_{ns\ -}$ » (« $K_{ns\ base}$ » x 0.1) and « $K_{ns\ --}$ » (« $K_{ns\ base}$ » x 0.01).

4.1. Extent of the valley influence

For quantifying the role of a valley on the overburden behaviour, it is necessary to be able to estimate the distance where the valley disturbs stresses in the medium. Figure 3 shows the maximum perturbation rate of three stresses (expressed in % in relation to initial stresses). Initially, the valley/tray limit is set for a perturbation rate of 2% in relation to initial stresses. Beyond this zone, the geomorphology corresponds to a tray situation.

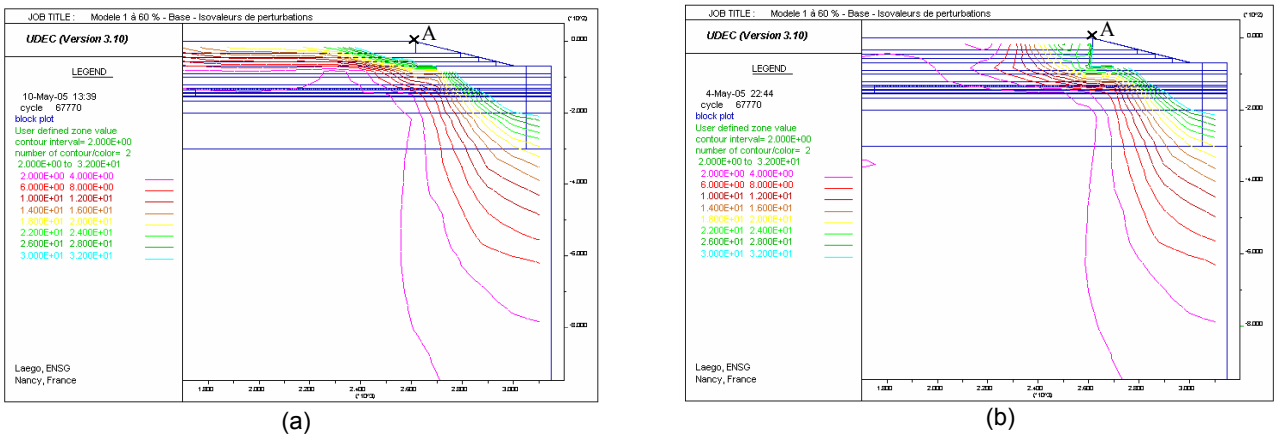

Figure 3: Maximum perturbation rate of stresses in relation to initial stresses for the « $K_{ns\ ++}$» (a) and « $K_{ns\ --}$ » (b)

The perturbation zone becomes more restricted when stiffnesses become low. Various distances found on the surface, for a rate of 2%, are specified in table 2. They are calculated from the slope rupture line (point A).

Table 2: Influence distances fixed to 2% according to different values of joint stiffness

Joint stiffness	Influence distance in relation to the valley
$K_{ns\,--}$	425 m
$K_{ns\,-}$	835 m
$K_{ns\,base}$	975 m
$K_{ns\,+}$	1020 m
$K_{ns\,++}$	1360 m

Low stiffnesses facilitate movements and can generate released stresses within the matrix. With high characteristics, stresses will be more compressive and blocks less constrained to move toward the empty space created by the valley. Therefore influence distances will be larger for « $K_{ns\,+}$» and« $K_{ns\,++}$» cases.

4.2. Plastic zones induced by the valley according to joint stiffness

The study of plastic zones repartition (figure 4) developed along layer limits (joints) and in the rock material allows us, at a first time, to approach of the mechanism associated to the valley excavation according to each joint stiffness set.

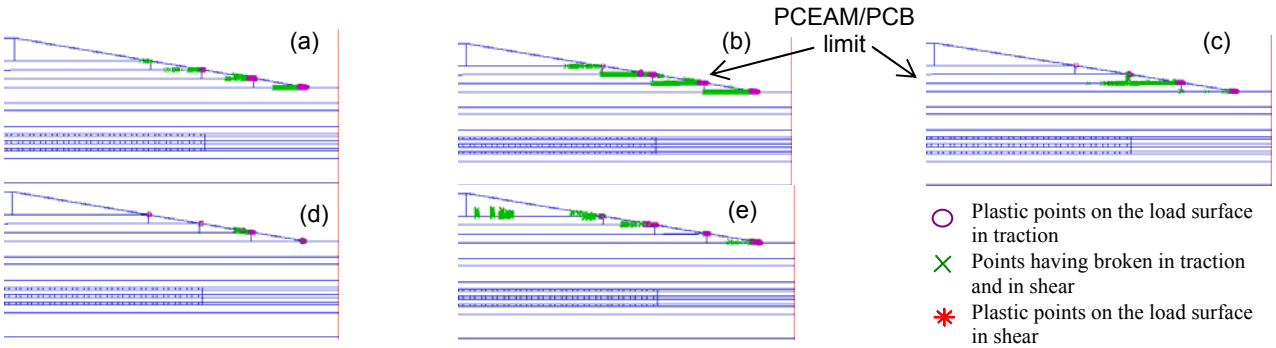

Figure 4: Plastic zones repartition for $K_{ns\,++}$ (a), $K_{ns\,+}$ (b), $K_{ns\,base}$ (c), $K_{ns\,-}$ (d) and $K_{ns\,--}$ (e) cases

In the reference case (« K_{ns} » stiffness set), there is an important plastification near the PCEAM/PCB limit.

If joint stiffness are increased by a factor of 10 and 100 (« $K_{ns\,+}$ » and « $K_{ns\,++}$ »), in the « $K_{ns\,+}$ » case, plastic zones appear at the layer limit level. All stiffnesses were multiplied by a factor 10 involving, therefore, more limited displacements and more high stresses along the layer limits. This plastic zone repartition is explained by the presence of shear failure occurring along joints. These failures initiate when the shear criterion $\tau_p = \sigma_n \mathrm{tg}\phi_j + C_j$ is reached, where Φ_j and C_j correspond to the joint friction angle and joint cohesion. The shear stress, on the joint, is limited by the peak value and a shear important displacement appears along the discontinuity. Proximity to the joint and in the matrix, the horizontal stress is constrained (limited also by the shear failure criterion for rock material) leading to important displacements and deformations and the appearance of plastic zones in the matrix. If joints behave elastically (by increasing the friction angle and cohesion), these broken zones would not occur on both sides of the discontinuity.

For the « $K_{ns\,++}$ » case, plastic zones are reduced especially at the PCEAM/PCB limit. At this stage, the joint stiffness is so much higher (100 times larger) than movements are impossible further to the valley formation. From a physical point of view and compared to basic values, joints are more compressed. This does not correspond to reality, because near the valley, joints release and deteriorate, therefore increase their deformability.

Plastic zones do not develop any more in layer limits in the « $K_{ns\,-}$» case. Movements are facilitated (stiffnesses 10 times smaller than basic stiffnesses) and stresses are weaker. Layer limits do not break in shear and do not lead failures in zones on both sides of these limits.

Finally in the « $K_{ns\,--}$» case, vertical fractures appear in Jaumont limestone within rock matrix and on the valley side in PCGC. The presence of plastic zones (assimilated to vertical fractures in rock matrix) seems to be the result of an important dextral and sinistral movement on both side of the joint segments (facilitated by low stiffnesses) creating a tensile failed zone and leading to the propagation of vertical fractures in the matrix.

4.3. Relative tangential and normal displacements according to stiffnesses

The main mechanism of movement for all case of sensitive analysis on joint properties, corresponds to a dextral tangential displacement. High values of relative shear displacement are associated to the set of low joint stiffness and low values of shear stress (figure 5). For the « $K_{ns\,--}$» case, a sinistral displacement appears along the joint at 32 m in the medium (surrounded by the red dotted line, figure 5b). This is also related to the apparition of plastic zones perpendicular to joint in JCB layer. The normal displacement or joint opening increases when joint stiffness became more and more low. The opening passes in order to 4.7 µm for the « $K_{ns\,++}$» case from 2.5 cm for the « $K_{ns\,--}$» case at the JCB/PCGC limit.

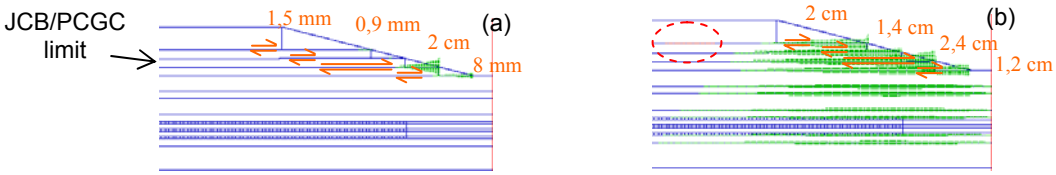

Figure 5: Relative tangential displacement for $K_{ns\,++}$ (a) and $K_{ns\,--}$ (b) cases

4.4. Horizontal and vertical stresses within layers according to joint stiffness

The study of horizontal stress profiles (for depth of 16 m, figure 6a) according to joint stiffness shows that when the valley is excavated, the horizontal stress releases when approaching the valley. The more stiffnesses are low, the less the stress is compressive. For the « $K_{ns\,--}$» case, the horizontal stress is subject to a sudden compression in relation to with the apparition of plastic zones (§ 4.2) within the JCB block rock material (stress variation in order to 0.45 MPa). The vertical stress (figure 6b) is subject to, for all depths, a decrease near the valley. Only the stress in the « $K_{ns\,--}$» case indicates an oscillation between compression and release because of the presence of plastic zone in the layer.

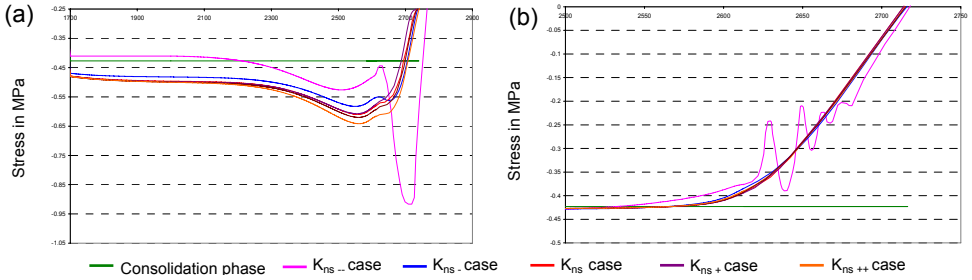

Figure 6: Horizontal (a) and vertical (b) stress profiles at a depth of 16 m (in JCB limestone)

For the other profiles in depth, the horizontal and vertical stresses also release in the vicinity of the valley with an amplitude which increases with the depth.

5. Case of an exploitation in depth: basic case

Several cases are considered: an exploitation situated under the tray (fig 9a), an exploitation situated alongside the valley (figure 9b) and an exploitation situated under the valley (figure 9c).

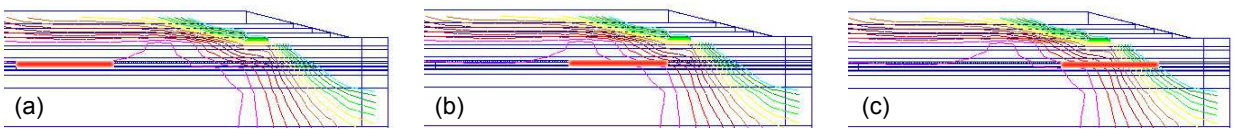

Figure 9: Different exploitation cases

The mine under the tray takes place in an undisturbed zone (rate of stress variation less than 2%). The situation is different for the mine alongside the valley where the exploitation is situated in a 7% disturbed zone at the most. The last mine under the valley takes place in a completely disturbed

zone, due to the valley presence, with a rate varying between 2% and 32%. Thus, only the mine under the valley positions completely in the perturbation zone unlike the both others.

5.1. Relative tangential and normal displacements

On both sides of the mine, the tangential displacement induced in the overburden is both dextral and sinistral as shown in figure 10a. The tangential displacement induced ($U_{s\ exploitation} - U_{s\ excavation}$) by the exploitation under valley (case a), is more important than the both others cases, in PCEAM/PCB limit (figure 10b). For exploitations under tray and alongside the valley, the induced displacement is the same (7.18 10^{-5} m). The exploitation alongside the valley (case b) takes place finally in a not very disturbed zone by the valley even if the end of mine is excavated in a 7% disturbed zone in relation to the initial stress state. It causes in the overburden the same displacement as in the case of the mine under tray. On the contrary, for the mine under valley, the maximum tangential induced displacement recorded is of 7.78 10^{-4} m at the end of exploitation (ten times more).

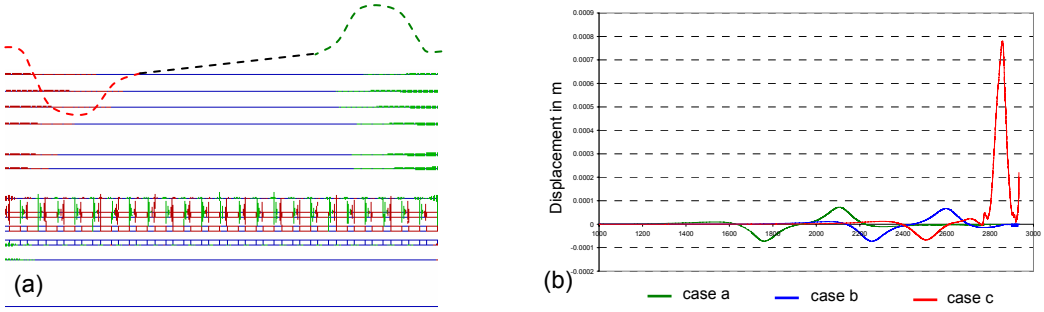

Figure 10: Relative tangential displacement

The normal displacement (fig 11a), induced by exploitations, shows a double flexion trend. It is equivalent for mines situated under tray and alongside the valley as well as the tangential displacement (fig 11b). The maximum closure, in mine edge, is of 1.5 10^{-5} m and the opening of 1.8 10^{-5} m. The exploitation under valley involves a joint opening of 2.15 10^{-5} m and showing always this double flexion trend where the magnitude is affected by the proximity of the valley.

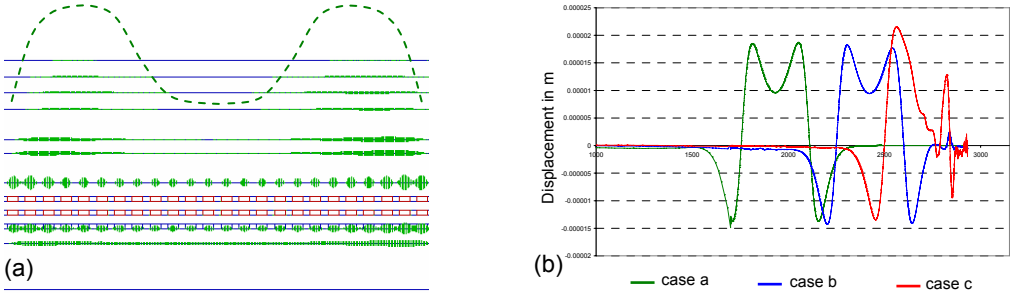

Figure 11: Relative normal displacement

At the start (without exploitation), the influence zone was defined for a stress perturbation rate of 2% (i.e. a disturbed zone until 975 m). In the presence of exploitation, the tangential and normal displacement shows that this zone must be considerably reduced, until 250 m about in the massif corresponding to a perturbation rate of 8%. This confirms that the starting criterion fixed to 2% was too large for estimating with significant and reasonable manners of the valley influence.

6. Influence of vertical fracture during the excavation valley phase

The introduction of vertical fracture aspires more to the reality even if the objective here, is not to represent it completely. The valley induces the development of fractures which are going to be more important at the approach of valley side, due to the release created by the empty space.

6.1. Influence valley zone: case of basic joint stiffness values

The vertical fracture introduction leads to a reduction of the influence valley zone (figure 12).

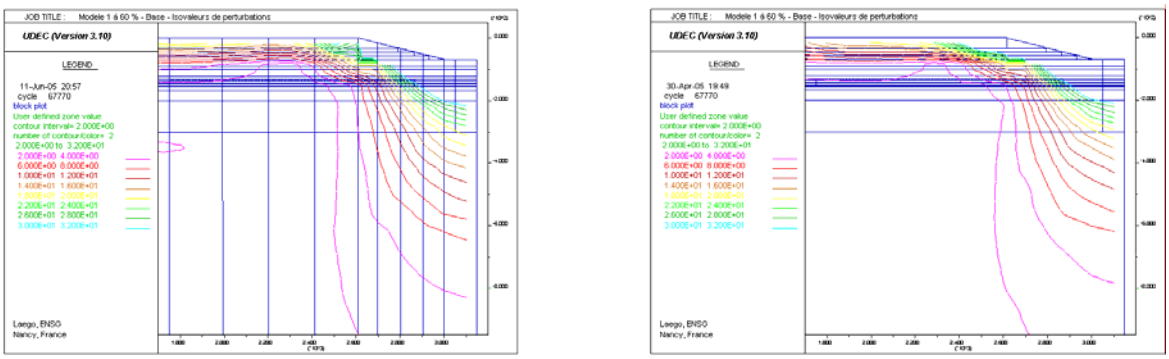

Figure 12: Influence valley zone in the case of basic stiffnesses

Vertical fractures seem to induce important displacements along vertical and horizontal joints synonymous with less compressive stresses allowing blocks to move more easily toward the empty space created by the valley. With this first analysis, the introduction of vertical fractures in the medium seems to release the sedimentary overburden.

6.2. Horizontal and vertical stresses in fractured and unfractured overburden

The horizontal stress induced by the valley excavation is less compressive (0.06 MPa), in the overburden, in fractured medium. This difference between the fractured and no fractured medium is more marked near the surface (0.11 MPa) what indicates that, superficially, the vertical fracture has a more significant effect on the horizontal stresses. Vertical stresses behave with the same manner as horizontal stresses in the sense of less compressive release than in the un fractured case in the vicinity of the valley.

6.3. Relative tangential and normal displacements in fractured and unfractured overburden

Tangential and normal displacements in layer limits are more significant in fractured medium. In the JCB/PCGC limit, the maximal displacement is five times more important (7.3 mm/ 1.4 mm) while in the PCGC/PCEAM, it is 2.5 times higher (3.8 cm/2.3 cm). An opening and a sinistral displacement appear along vertical fractures and which becomes weaker in depth. These displacements are all the more important as fractures are near the valley. Nevertheless it is low (tenth of millimetre at best) probably due to stiffnesses of vertical joints which are too high to involve large displacements along vertical fractures. All the same, this total increase of displacements is the result of a more released overburden in the fractured medium (§6.2).

6.4. Plastic zones developed in fractured and unfractured overburden

The plasticization developed along layer limits (fig 13) is more important in the fractured medium than in the no fractured medium. The failure criterion is reached more quickly in the fractured medium near the joint (because of not very compressive stresses and important tangential displacements) with a more important number of plastic zones.

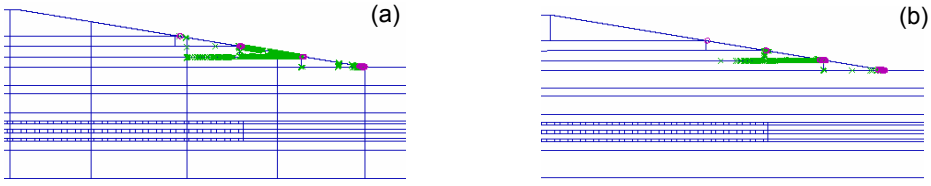

Figure 13: Plastic point repartition in fractured medium (a) and unfractured medium (b)

7. Valley influence and fractured medium in terms of stiffness on the overburden

The analysis of displacement and stress fields shows how all of the overburden limestone (consisting of a stiff bedrock) in the vicinity of the valley are subjected to the action of a vertical fracture set. The involved phenomena must be expressed into stiffness terms of overburden. Initially, it was estimated, in an intuitive way, that a free slope and the vertical fracture could have a tendency to reduce the overburden massivity. For the tray situation, the fracture is not well expressed; the corresponding overburden stiffness must be increased.

7.1. Displacements in the overburden

The tray situation can exist only at a certain distance of the slope. Initially, this situation is reached at approximately the distance of 975 m in comparison to the slope failure line (basic values of joint stiffness and a perturbation rate of 2%). This distance is variable according to the mechanical discontinuities properties and finally can be greatly reduced as seen in the paragraph 5.1 (250 m compared to 975 m in the basic case). In this zone, stresses and displacements are more released and more important. Figure 14 shows isovalues of displacements observed in the model.

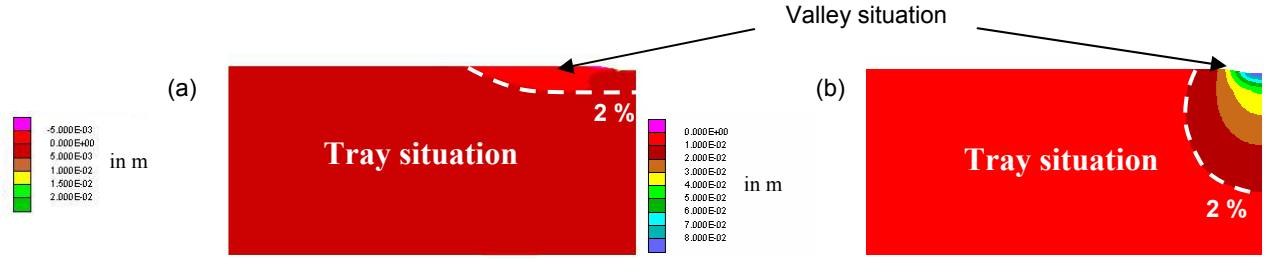

Figure 14: Horizontal (a) and vertical (b) displacement behind the valley excavation

The examination of horizontal displacement (figure 14a) shows that the observed displacement (5 mm) corresponds to the perturbation zone fixed initially to 2%. The vertical displacement (figure 14b) also underlines this zone and corresponds to movements of about 1 to 2 cm. These displacements allow in a first time to confirm the distinction between the tray and valley situation. Moreover in terms of massivity, these displacements are synonymous of an overburden less constrained near the valley and thus less stiff. This last remark comes to confirm that a free slope reduces the overburden massivity.

7.2. Vertical fracture

Harrison & Hudson (1997) have shown that the fracture had a tendency to reduce the massivity of a medium expressed through the homogeneous deformation modulus E_m:

$$E_m = \frac{\sum_i t_i}{\sum_i \frac{t_i}{E_i}} \quad \text{unfractured strata} \qquad (2)$$

$$E_m = \frac{\sum_i t_i}{\sum_i t_i \left(\frac{1}{E_i} + \frac{\lambda_i}{E_{di}} \right)} \quad \text{fractured strata} \qquad (3)$$

where λ_i corresponds to the frequency of fractures and E_{di} to the fracture stiffness in the layer i. The additional term of equation 3, λ_i/E_{di}, shows that the fractures have a tendency to reduce the homogeneous rock mass modulus, thus to weaken the stiffness in the rock unit.
The induced horizontal displacement (figure 15) by the valley excavation is more significant for overburden in the fractured medium than in the unfractured strata. In both cases, the overburden is subject to a displacement of 5.10^{-3} m with the only difference that in the fractured medium, this displacement stretches more laterally in the massif.

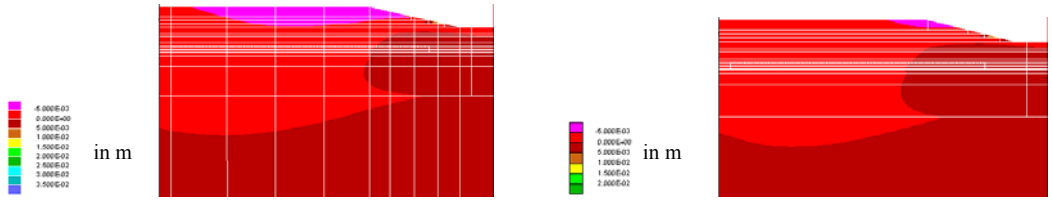

Figure 15: Horizontal displacement in fractured and unfractured medium

The vertical displacement (figure 16) is too more important in the fractured medium than in the unfractured ones. In the overburden, the valley induces a vertical displacement of about 10^{-2} to 2.10^{-2} m for the case without fractures. In the fractured medium, this same displacement reaches in the overburden a value of 10^{-2} to 4.10^{-2} m.

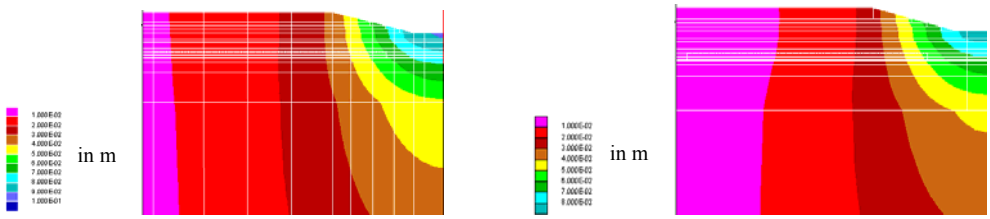

Figure 16: Vertical displacement in fractured and unfractured medium

The analysis of these displacement fields really seems to indicate that the presence of vertical fracturing causes important movements in layers, in connection with the less compressive stresses recorded (§6.2), and seems still more to reduce the massivity overburden. This is approached below in terms of strain energy balance.

8. Energy balance

Usually strain energy is stored within a block when the block is deformed under load. In the absence of energy dissipations, such as from friction or yielding, the strain energy is equal to the work done on the block by external loads. It is equal to the area under the stress-strain curve, and is a measure of the toughness of a block. The mechanisms noticed through these modellings (released stresses, displacements, plastic zones), are accompanied by a more or less important dissipation of energy. The total energy released correspond to the total dissipated strain energy in material (U_c), the total change in potential energy of the system (U_b), the total dissipated energy in joint shear (W_j) and the total dissipated work in plastic deformation of intact rock (W_p). Therefore if energy dissipations are weak in the overburden; this will be an indicator of a stiff behaviour.

8.1. Unfractured strata medium

Table 3 shows different energy dissipations between the initial state (consolidation phase in of terms of Itasca codes) and excavation phase:

Table 3: Dissipated energy according to stiffnesses between the initial state and excavation phase

	Kns --	Kns -	Kns	Kns +	Kns ++
Material strain energy U_c (J)	1563	1395	1453	1443	1455
Potential energy U_b (J)	82.63	74.17	75.76	75.24	75.58
Friction work W_j (J)	0.1739	0.0857	0.1281	0.1069	0.1064
Plastic strain work W_p (J)	$8.20.10^{-3}$	$7.25.10^{-4}$	$1.75.10^{-3}$	$1.45.10^{-3}$	$3.05.10^{-4}$
Total energy released (J)	1646	1435	1529	1518	1530

The total dissipated strain energy in material is important for the « $K_{ns\ --}$» case (1563 J) and quasi-equivalent for the other stiffnesses (≈ 1450 J) except for the « $K_{ns\ -}$» case (1395 J). The total change in potential energy is more important for the « $K_{ns\ --}$» case due to the important displacements (§4.3). Plastic strain energy (W_p) describes the deformability of the blocks. Energy is dissipated

through plastic work equivalent to irreversible deformation in the rock blocks. With the exception of « $K_{ns\,++}$» case (joints too compressed, §4.2), this energy is weaker for the « $K_{ns\,-}$» case than the other cases (figure 17a). In other words, the deformability of blocks is weaker for the « $K_{ns\,-}$» case (emphasized by the presence of few plastic points developed in layer limits §4.2).
With a less deformability or a more constrained medium, the total released energy (figure 17b), between the initial state and the excavation phase, is less important for the « $K_{ns\,-}$» case (1435 J). Therefore in this last modelling, energy dissipations are weak involving a stiffer overburden than for the other cases.

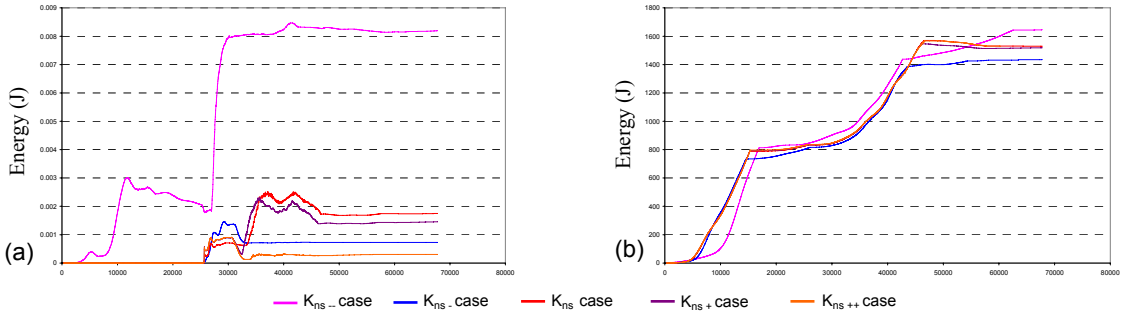

Figure 17: Evolution of total dissipated work in plastic deformation (a) and total energy released (b)

8.2. Comparison between the unfractured and fractured strata medium

Table 4 shows energy dissipations between the fractured medium and the unfractured medium:

Table 4: Dissipated energy in fractured and unfractured medium

	Fractured	No fractured
Material strain energy U_c (J)	1457	1453
Potential energy U_b (J)	300.5	75.76
Friction work W_j (J)	0.2167	0.1281
Plastic strain work W_p (J)	$8.25\ 10^{-3}$	$1.75\ 10^{-3}$
Total energy released (J)	1754	1529

The total dissipated strain energy in material is the same for both cases due to stiffnesses of vertical fractures which are too high as seen in §6.3. Even if displacements are weak along vertical joints, general displacements within rock blocks involve a released potential energy four times more important in the fractured medium in accordance with displacements observed in paragraph 7.2. Plastic strain energy does not contribute with a significant manner on the total released energy (few thousandth of joule) but it gives an idea of the deformability of the blocks. It is five times higher in the fractured medium which indicates that the fractured medium is more deformable than the unfractured medium. Consequently, the fractured medium releases an important total energy (1754 J) in comparison with the no fractured medium (1529 J). These last observations confirm the assumption that the overburden is more released with the presence of vertical fractures.

9. Conclusion

This methodology allows fixing a distance from which the valley disturbs stresses in the overburden. This distance is variable according to joint stiffnesses. For the basic case, it was fixed at 250 m (from the slope failure line) corresponding to a perturbation rate of 8% in relation to initial stresses. Beyond this zone, the geomorphologic situation is a tray situation. During the valley excavation and according to stiffnesses, stresses release, the plastic points and displacements (shear and normal) appear along discontinuities. The introduction of vertical fractures accentuates displacements, stresses are more released and plastic zones are more numerous. These induced phenomena act on the overburden behaviour in terms of stiffness. The general study of displacements and energy balances show that near the valley, the overburden is less massive than in tray situation. This release is more important in the presence of vertical fractures.

10. References

Bandis S.C., Lumsden A.C. and Barton N.R. (1983). *Fundamentals of rock joint deformation*, Int. J. Rock Mech. Min. Sci & Geomech. Abstr., 20, 249-268.

Bennani M., Homand F. (2004). *Les formations de couverture au droit des zones d'aléa d'effondrement brutal*, rapport LAEGO-GEODERIS, R2004-002_LG.FH.GEO.PSI.RPRE.04.0059.C, juillet 2004.

Harrison J.P., Hudson J.A. (1997). *Engineering Rock Mechanics, Part 2: Illustrative Worked Examples*, Pergamon, 506 pages, 1997.

Homand F. (2004). *Etude des formations de couverture au droit de zones à risque*, rapport GEODERIS, LG.FH.GEO.PSI.RPRE.03.0248.A, juillet 2004.

Kulatilake P.H.S.W., Ucpirti H., Wag S., Radberg G. and Stephansson (1992). *Use of the distinct element method to perform stress analysis in rock with non-persistent and to study the effect of joint geometry parameters on strength a deformability of rock masses*, Rock Mech. and Rock Engng., 25, 253-284.

Merrien-Soukatchoff V., Omraci K. (2000). *Détermination des conditions aux limites pour un calcul de stabilité de talus*, Revue Française de Géotechnique, 92, 3ème trimestre 2000, 31-39.

Thoraval A. (2000). *Etudes réalisées dans le cadre du GISOS et cofinancées par les fonds du CIADT pour 1999-2000*, rapport INERIS ref. DRS-00-23744/RN01, rapport GISOS n°28, décembre 2000.

Tincelin E., Sinou P. (1962). *Effondrements brutaux et généralisés – Coups de toit*, Revue Industrielle et Minérale, avril 1962.